JOURNAL OF
EMERGING INVESTIGATORS

Article

De novo design of a dual-target inhibitor against tau phosphorylation and acetylation for Alzheimer's therapy

Qiting (Annie) Zhou[1], Ellen Wang[1]
[1] Plano West Senior High School, Plano, Texas

SUMMARY

Alzheimer's disease (AD) is a progressive neurodegenerative disorder affecting approximately 7 million Americans and is the most common form of dementia. The pathological hallmarks of AD are the accumulation of amyloid-beta plaques and neurofibrillary tangles composed of tau protein that have undergone abnormal post-translational modifications (PTMs). While tau hyperphosphorylation has been extensively studied, tau acetylation occurs at fewer sites and remains comparatively understudied, representing a critical gap in understanding AD progression. In this study, we investigated how tau acetylation influences aggregation relative to phosphorylation and evaluated whether a brain-permeable retro-inverso peptide could be rationally designed to inhibit both glycogen synthase kinase-3β (GSK3β), a major tau kinase, and the tau-acetylating enzyme p300. We hypothesized that acetylation would promote aggregation less strongly than phosphorylation due to its lower reported prevalence. To test this, we computationally modeled full-length human tau and generated native, phosphorylated, acetylated, and dual-modified variants at AD-associated residues. Aggregation propensity and structural flexibility analyses revealed that acetylation significantly increased aggregation and conformational instability, comparable to phosphorylation, while dual modification produced additive destabilizing effects. We then designed a retro-inverso peptide inhibitor, RI-GSK, and evaluated its binding to GSK3β and p300 using molecular docking. RI-GSK demonstrated stronger predicted binding affinities than several AD therapeutics pursued in clinical trials, along with favorable pharmacokinetic properties and predicted blood–brain barrier permeability. Although experimental validation is required, these findings suggest that tau acetylation may contribute substantially to pathogenic aggregation and highlight dual-target retro-inverso peptides as a promising strategy for future AD drug development.

INTRODUCTION

Approximately 7 million Americans are currently living with Alzheimer's, and by 2050, this number is projected to rise to 13 million (1). Alzheimer's disease (AD) is a progressive neurodegenerative disorder marked by memory loss, cognitive decline, and widespread neuronal dysfunction (1). Its pathology includes several hallmark features: amyloid-beta plaques (protein deposits between neurons), chronic inflammation (immune-related tissue damage), synaptic loss (breakdown of neuronal connections), and neurofibrillary tangles (abnormal protein clumps within neurons) composed of aggregated tau protein (2). AD is part of a broader class of neurodegenerative diseases known as tauopathies, which also includes progressive supranuclear palsy (PSP), corticobasal degeneration (CBD), and frontotemporal dementia with tau pathology (FTD-tau), all characterized by pathological aggregation of tau protein (2). Tau normally stabilizes microtubules and supports axonal transport, especially in adult human neurons where the 2N4R isoform is dominant. Out of the six splice variants of tau protein, the 2N4R isoform (441 aa) is the most commonly implicated splice variant in Alzheimer's (3). Tau function is tightly regulated by post-translational modifications (PTMs), chemical changes made to proteins after they are synthesized, most notably phosphorylation (addition of phosphate groups) and acetylation (addition of acetyl groups) (3,4).

Phosphorylation of tau has been extensively studied in AD. Under normal conditions, phosphorylation at select serine and threonine residues helps regulate microtubule dynamics (5). However, in AD, tau becomes hyperphosphorylated at dozens of sites, including S199, S202, T205, S214, S262, S396, and S404, which reduces microtubule binding and increases fibril formation (6). Glycogen synthase kinase-3β (GSK3β) is one of the major kinases responsible for this hyperphosphorylation (4, 5).

Acetylation of tau, by comparison, is a less well-characterized, but increasingly relevant, PTM. Tau can be acetylated by histone acetyltransferases such as p300 (EP300) and CBP, especially at lysine residues within the microtubule-binding repeats and KXGS motifs (e.g., K274, K280, K281, K290, K298) (6). Some studies suggest these modifications impair tau clearance and promote aggregation, but the overall contribution of acetylation relative to phosphorylation remains unclear (7). In the human brain, phosphorylation of tau is more widespread and has been mapped at dozens of sites, while acetylation has been reported at a smaller number of lysines concentrated in microtubule-binding repeats and regulatory motifs (6, 7). Dual modification at both phospho- and acetyl-sites has been observed in tau from AD brains, suggesting that these PTMs can coexist on the same molecule (8). This raises the question of whether acetylation makes a comparable contribution to aggregation or mainly acts as a secondary modifier. Both PTMs also have physiological roles in normal tau function: phosphorylation helps regulate axonal transport, and low-level acetylation influences protein interactions and turnover (9). Any therapy aimed at reducing these PTMs must account for both pathological and normal functions.

Because AD involves multiple abnormal PTMs occurring

https://doi.org/10.59720/25-250

simultaneously, therapies directed at only one modification may be insufficient (9). Current FDA-approved AD drugs, such as cholinesterase inhibitors (donepezil, rivastigmine, galantamine) and NMDA receptor antagonists (memantine), do not directly target tau-modifying enzymes (10). To bridge this gap, our goal was to design a drug that could target the enzymes responsible for both tau phosphorylation and acetylation. We chose retro-inverso peptides, synthesized from D-amino acids in reversed sequence order, as they are known to offer improved stability and protease resistance, and can be easily engineered to interact with multiple targets (11).

In this study, we investigated whether tau acetylation increases aggregation to a similar extent as phosphorylation and whether a dual-target retro-inverso peptide can be rationally designed to bind both the GSK3β ATP-binding site and the p300 HAT domain (the site responsible for histone acetyltransferase catalysis) with high affinity and favorable drug-like properties. We hypothesized that acetylation would not increase aggregation as strongly as phosphorylation and that a dual-target retro-inverso peptide could achieve stronger binding than existing small-molecule modulators of these enzymes. To answer these questions, we used an *in-silico* pipeline. We modeled PTM-specific variants of full-length 2N4R tau, quantified aggregation and flexibility using AGGRESCAN4D and CABS-Flex, and applied RFdiffusion to design retro-inverso peptide candidates that could bind both GSK3β and the p300 HAT domain. We used docking, molecular dynamics simulations, and ADMET predictions to evaluate target engagement and drug-like properties. This computational approach allowed us to systematically compare the effects of phosphorylation and acetylation and to explore dual-target inhibitor design without requiring immediate access to wet-lab experiments. Our findings revealed that acetylation significantly increases tau aggregation, and we successfully designed a dual-target peptide with favorable predicted binding and brain permeability properties.

RESULTS

Acetylation significantly increases tau aggregation and instability

Our goal was to determine the role of acetylation in tau protein aggregation. To accomplish this, we modeled four forms of full-length human 2N4R tau (441 aa): native, phosphorylated, acetylated, and dual-modified. We selected phosphorylation sites (S199, S202, T205, S214, S262, S396, S404) and acetylation sites (K274, K280, K281, K290, K298) based on their documented involvement in AD and other tauopathies (6, 7, 12). These sites fall within or near microtubule-binding repeats and KXGS motifs, regions known to regulate tau aggregation (15).

To measure aggregation propensity, we used AGGRESCAN4D, a computational tool that predicts how likely protein regions are to form aggregates. AGGRESCAN4D revealed that phosphorylated and acetylated tau both exhibited significantly higher aggregation scores than native tau, indicating greater tendency to clump together and form neurofibrillary tangles (**Figure 1**; two-way ANOVA, $p < 0.0001$). All modified variants, including the singly phosphorylated, singly acetylated, and dual-modified forms, differed significantly from native tau (**Figure 1**). The dual-modified variant showed the highest aggregation scores, suggesting additive effects **(Figure 1).**

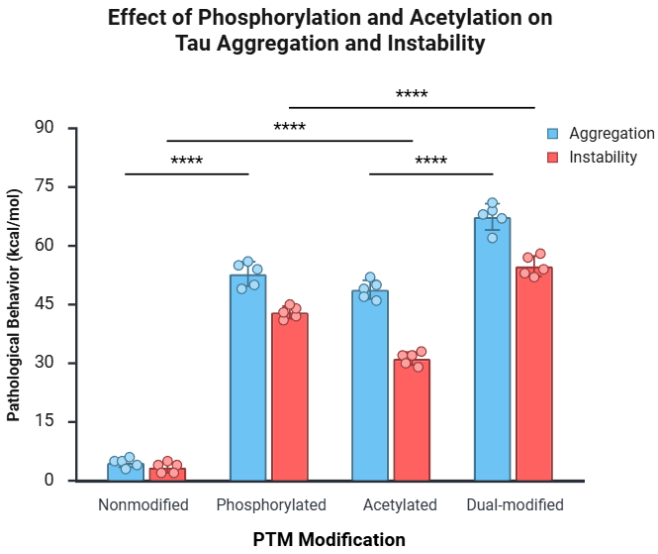

Figure 1: Acetylation and phosphorylation significantly promote tau aggregation and instability, while dual-modification poses additive effects. Bar chart showing mean ± SD aggregation scores from AGGRESCAN4D (blue) and instability indexes from CABS-Flex analysis (red) for native (nonmodified), phosphorylated, acetylated, and dual-modified tau variants. Two-way ANOVA, ****$p < 0.0001$, $n = 5$ independent simulations per variant.

We next assessed structural flexibility to understand whether these modifications also destabilize tau's structure. We used CABS-Flex, a coarse-grained flexibility simulation tool, which calculates residue-level root mean square fluctuation (RMSF). RMSF is a measure of how much each part of the protein moves during simulation, with higher values indicating greater local motion and reduced structural stability (14). Acetylated tau showed larger RMSF values in the microtubule-binding region than native tau, indicating reduced stability **(Figure 1)**. Phosphorylated tau displayed a similar pattern, and the dual-modified variant had the highest RMSF overall. We interpreted higher RMSF as increased local flexibility and decreased structural stability, consistent with the increased aggregation scores from AGGRESCAN4D, which predicts residue-level aggregation propensity (16).

De novo design of a dual-target retro-inverso peptide inhibitor

To develop a therapeutic candidate that could simultaneously target both phosphorylation and acetylation, we generated 50 retro-inverso peptide candidates using RFdiffusion, a deep-learning-based protein design framework (13). We obtained crystal structures of GSK3β (PDB ID: 1I09) and the p300 HAT domain (PDB ID: 3BIY) from the Protein Data Bank. The design constraints targeted two enzyme pockets: the ATP-binding cleft of GSK3β (where the enzyme binds ATP to transfer phosphate groups to tau) and the acetyl-CoA/substrate-binding groove of the p300 HAT domain (where acetyl groups are transferred to tau lysines). We chose these specific binding sites because they represent the catalytic centers where each enzyme modifies tau. Retro-inverso scaffolds were chosen because of their known stability, protease resistance, and potential to cross the blood-brain barrier.

https://doi.org/10.59720/25-250

Design	Mean MPNN score ±0.05	Model confidence (pLDDT) ±0.05	pTM interaction score ±0.1	Interface error score ±0.1	Backbone RMSD (Å) ±0.2
1	1.356286	0.653657	0.833429	20.64283	16.45045
2	1.279463	0.669412	0.815802	21.01308	14.98898
3	1.276794	0.735479	0.809118	21.99433	22.74553
4	1.313278	0.856882	0.724513	21.30411	22.90536
5	1.267293	0.842744	0.735538	20.95965	21.2724
6	1.289019	0.749019	0.735679	20.32517	21.91949
7	1.300481	0.720414	0.631014	20.36796	24.46487
8	1.325244	0.858397	0.752345	20.6638	21.5336
9	1.307991	0.681558	0.527006	20.62288	12.71169
10	1.318175	0.836419	0.676832	19.0632	24.61073

Table 1: RFdiffusion and docking-based evaluation of the top ten retro-inverso peptide candidates out of the initial 50 RFdiffusion candidates ranked by structural and interaction metrics. Mean sequence design score (MPNN) reflects how compatible the amino acid sequence is with the designed backbone. Model confidence (pLDDT) is the predicted local distance difference test score, with higher values indicating higher structural confidence. PTM interaction score and interface error score summarize predicted interaction quality with the target surfaces

We evaluated the top ten RFdiffusion designs using several model-derived metrics (**Table 1**). The pLDDT score reflects local model confidence, with higher values indicating more reliable backbone geometry. The MPNN score summarizes how well the designed sequence fits the predicted backbone. The interaction error score and the predicted Template Modeling score (pTM) estimate the predicted alignment error between the two protein interfaces and the quality of the protein's folded structure, respectively, while RMSD reports structural variability across predicted models. We considered the most promising candidates as the ones with higher pLDDT, favorable interaction scores (lower interaction error score and higher pTM interaction score), and moderate RMSD (indicating a stable but not overly constrained conformation). We ultimately selected RI-GSK because it combined relatively high pLDDT and interaction scores with compact geometry, suggesting a good balance between structural stability and the ability to engage both pockets reliably **(Figure 2).**

RI-GSK showed favorable binding to GSK3β and p300 compared with known inhibitors

To evaluate whether RI-GSK could effectively bind to our target enzymes, we performed molecular docking experiments. Molecular docking is a computational method that predicts how well a small molecule or peptide fits into a protein's binding pocket and estimates the strength of that interaction. We used AutoDock Vina, a molecular docking program, to test RI-GSK's binding (16). The results showed that RI-GSK bound strongly to key residues within the ATP-binding cleft of GSK3β and the acetyl-CoA catalytic groove of p300 HAT domain (**Figures 3 and 4**). To contextualize these results, we compared the binding affinity of RI-GSK to both GSK3β and p300 with five small-molecule inhibitors pursued in AD clinical trials, including GSK3β inhibitors tideglusib, epigallocatechin gallate, methylene blue, and curcumin, which is also a p300 inhibitor along with salsalate (17, 18).

RI-GSK exhibited the most favorable (most negative) binding energies for both targets (**Figure 5**). Two-way ANOVA followed by Tukey's multiple-comparison test confirmed that RI-GSK bound significantly more strongly (adjusted $p < 0.01$ for all comparisons) to both the p300 HAT domain and the ATP-binding site of GSK3β than all comparator molecules (tideglusib, salsalate, EGCG, methylene blue, and curcumin) (**Figure 5**).

RI-GSK's binding energies to GSK3β and p300 did not differ significantly from each other (adjusted $p = 0.8049$), consistent with its multi-target design. To further validate the stability of these interactions, we performed molecular dynamics simulations using OpenMM, a GPU-accelerated molecular dynamics engine (19). These simulations model how protein-peptide complexes move and interact over time under physiological conditions. The simulations confirmed that the peptide-protein complexes maintained stable interactions throughout 50-ns trajectories, suggesting the binding would be maintained over biologically relevant timescales.

RI-GSK displayed favorable drug-likeness and brain permeability

Finally, we evaluated the pharmacokinetic and drug-likeness properties of the top peptide designs using SwissADME and ProTox-II, focusing on parameters relevant to central nervous system (CNS) drugs. RI-GSK satisfied common CNS-oriented filters for molecular weight, lipophilicity, topological polar surface area, and number of rotatable bonds (**Figure 6**). In general, small molecules that successfully reach the brain tend to have a molecular weight below roughly 500–600 Da, a logP between about 1 and 4, and a topological polar surface area below approximately 90 Å² (20). RI-GSK fell within all key parameter ranges, suggesting that its physicochemical properties are compatible with brain penetration.

SwissADME also reported a blood–brain barrier (BBB) permeability score of 4.96 out of six for RI-GSK. This score is a dimensionless, tool-specific index where values greater than four correspond to a high likelihood that a compound can cross the BBB and will be CNS-active (21). While the scale is not directly comparable to experimental permeability measurements, values in this range are often associated with compounds that reach the CNS *in vivo*. ProTox-II predicted a low toxicity class for RI-GSK and did not flag major structural alerts for common toxicophores. Taken together, these *in silico* results suggest that RI-GSK may have pharmacological properties consistent with CNS-active compounds, but

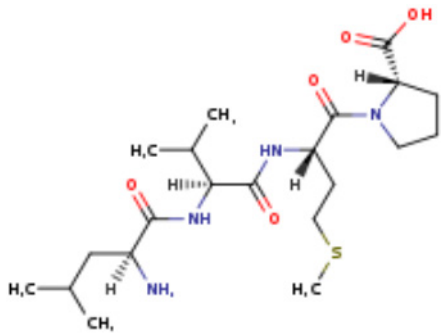

Figure 2: Chemical structure of the retro-inverso peptide RI-GSK. Six-residue peptide structure visualized using SwissADME. The structure shows D-amino acids in reversed sequence order, with hydrophobic residues (leucine and valine side chains shown in the structure) incorporated at solvent-exposed positions to enhance BBB permeability and drug-likeness.

https://doi.org/10.59720/25-250

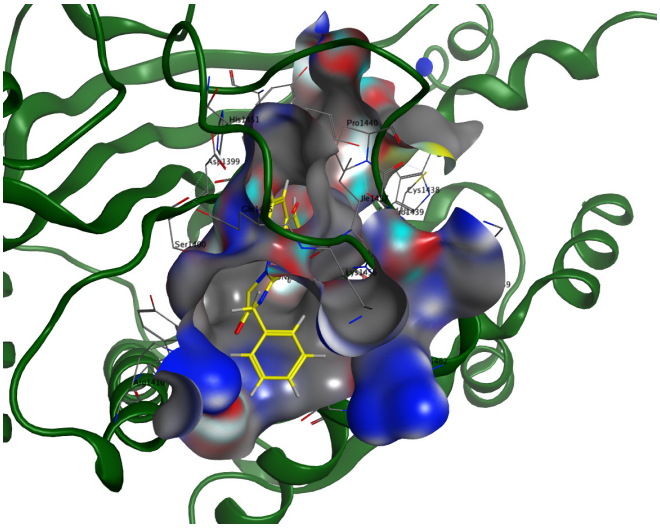

Figure 3: RI-GSK binding to the p300 HAT domain active site. Molecular docking model generated in BIOVIA Discovery Studio showing RI-GSK binding to key residues in the acetyltransferase's acetyl CoA substrate-recognition site illustrated in green (PDB ID: 3BIY).

experimental ADMET studies will be necessary to validate these predictions.

DISCUSSION

Tauopathies are a class of neurodegenerative diseases, including Alzheimer's disease (AD), progressive supranuclear palsy (PSP), corticobasal degeneration (CBD), and frontotemporal dementia with tau pathology (FTD-tau), that arise from a combination of abnormal post-translational modifications (PTMs), loss of microtubule stability, buildup of amyloid beta plaques, and progressive aggregation of tau into fibrillar structures (22). Much of the existing literature has focused on tau hyperphosphorylation as a major driver of aggregation, with extensive evidence linking phosphorylation at residues such as S202, T205, S262, S396, and S404 to reduced microtubule binding, conformational destabilization, and enhanced fibril formation (6, 23). Acetylation has been studied less thoroughly, but emerging work shows that p300/CBP-mediated acetylation at lysines within the microtubule-binding repeats can impair tau clearance, block ubiquitin-mediated degradation, and promote accumulation of aggregation-prone tau species (7, 24). Our modeling results are consistent with this growing body of evidence: in our system, acetylation increased aggregation propensity and structural flexibility to nearly the same degree as phosphorylation, and the dual-modified variant showed the strongest predicted instability. These behaviors align well with recent experimental findings that phosphorylation and acetylation can cooperate to accelerate tau misfolding (25). Because our work uses *in silico* modeling, these results should be interpreted as supportive rather than conclusive; experimental validation will be necessary to determine whether the predicted effects occur in biochemical or cellular systems. While AD is a secondary tauopathy characterized by both tau pathology and amyloid-beta plaques, our study focuses specifically on tau PTMs and aggregation mechanisms that are shared across tauopathies, making these findings most directly applicable to primary tauopathies where tau is the principal pathogenic driver and broadly relevant to understanding the tau component of AD.

Beyond PTM modeling, our study contributes to ongoing efforts to develop enzyme-targeted therapeutics for tauopathy. Several groups have investigated GSK3β inhibitors, including tideglusib and lithium derivatives, though clinical translation has been limited by toxicity, narrow therapeutic windows, or insufficient brain penetration. Similarly, p300/CBP inhibitors like salsate have been proposed as potential modulators of tau acetylation, but very few compounds have advanced beyond early preclinical studies. To our knowledge, no approved tauopathy therapy currently targets both phosphorylation and acetylation pathways simultaneously. Our work therefore adds a novel conceptual step: we show that a small retro-inverso peptide can be rationally designed to engage catalytic residues within both GSK3β and the p300 HAT domain, suggesting the feasibility of a dual-target strategy upstream of tau aggregation. This is in line with a broader shift in neurodegeneration research toward multi-target inhibitors, which have shown promise in various other disease areas such as oncology and metabolic disorders. At the same time, because docking and dynamics simulations are predictive tools, we cannot conclude that RI-GSK achieves biologically meaningful inhibition, and we avoid overstating therapeutic implications.

Importantly, the specific binding sites highlighted in our docking models represent functional regions of each enzyme. In GSK3β, RI-GSK inserts into the ATP-binding cleft and interacts with residues that coordinate phosphate transfer to substrates such as tau. In p300, RI-GSK binds within the acetyl-CoA and substrate-recognition groove, where acetylation of lysine residues—including several implicated in tauopathy—occurs. This site-specific positioning suggests a plausible mechanism by which RI-GSK could interfere with tau-modifying activity, but confirming this mechanism would require enzyme kinetics, competitive binding assays, and mutational analysis of catalytic residues.

Looking forward, several key experiments would be needed to evaluate RI-GSK or any dual-target peptide as a

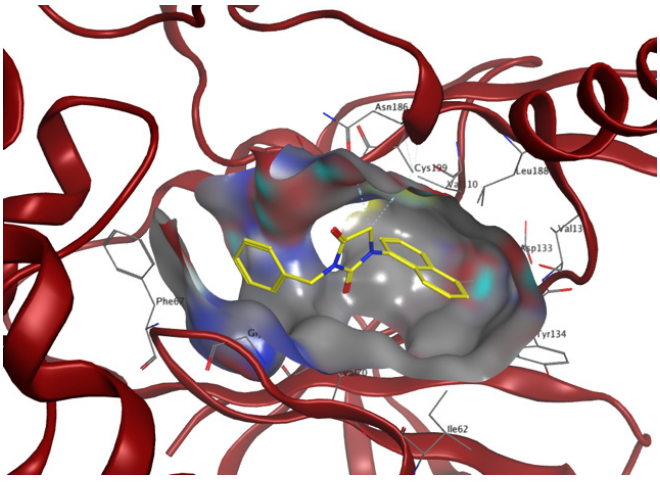

Figure 4: RI-GSK binding to the ATP-binding pocket of GSK3β. Molecular docking visualization in BIOVIA Discovery Studio highlighting interactions between RI-GSK (shown in yellow) and key GSK3β residues in the ATP-binding site shown in green (PDB ID: 1I09).

https://doi.org/10.59720/25-250

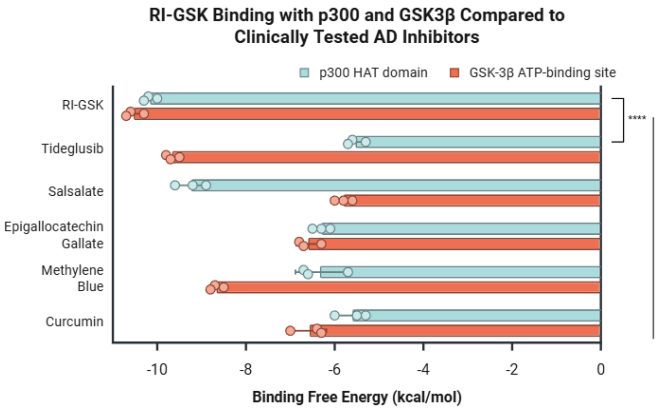

Figure 5: Binding energy comparison of RI-GSK and currently known Alzheimer's inhibitors targeting the GSK3β and p300 HAT domain. Bar graph showing mean ± SD binding energy (kcal/mol) calculated by AutoDock Vina for RI-GSK and five comparator inhibitors at both the p300 HAT domain and GSK3β ATP-binding site. Two-way ANOVA with Tukey's post-hoc multiple-comparisons test were conducted; RI-GSK showed significantly stronger binding than all comparator inhibitors at both targets (adjusted $p < 0.01$ for every pairwise comparison). n = 3 separate docking simulations were conducted for each inhibitor.

therapeutic candidate. *In vitro* kinase and acetyltransferase inhibition assays using purified GSK3β, p300, and recombinant tau could determine whether RI-GSK reduces phosphorylation or acetylation at specific pathological residues. Aggregation assays using full-length tau or microtubule-binding repeats could test whether the peptide slows fibril formation or alters oligomer structure. Cell-based models, such as tau-expressing neuronal cultures or induced pluripotent stem cell-derived neurons, could evaluate effects on tau stability, turnover, and aggregation under more physiological conditions. If these results were promising, *in vivo* testing in tauopathy mouse models would be essential to assess pharmacokinetics, biodistribution, blood-brain barrier permeability, toxicity, and behavioral or histological outcomes.

Finally, while our study focused on phosphorylation and acetylation, tau pathology is shaped by additional PTMs, including ubiquitination and SUMOylation. Ubiquitination is involved in proteasomal targeting, and several studies have shown that pathological tau species accumulate when ubiquitin-mediated clearance fails (19). Tau SUMOylation has also been reported to promote aggregation and interfere with degradation pathways (20). These findings suggest that targeting multiple PTMs simultaneously may more effectively modulate tau homeostasis than focusing on a single modification. Although our model does not include these PTMs, our results support the broader principle that tau dysfunction emerges from the combined influence of several upstream enzymatic pathways, and that multi-target approaches may ultimately prove more effective than single-pathway interventions.

In summary, our computational work suggests that acetylation may play a more substantial role in tau aggregation and instability than previously appreciated and demonstrates that a short retro-inverso peptide can be designed to engage two tau-regulating enzymes at functionally meaningful sites. These findings extend current knowledge and offer a set of mechanistic predictions and candidate molecules that can be tested experimentally. Ultimately, validating the therapeutic potential of dual-target inhibition will require extensive biochemical, cellular, and *in vivo* studies, but this work provides a promising starting point for such efforts.

MATERIALS AND METHODS

Tau Structure and Post-Translational Modification Modeling

The full-length human 2N4R tau isoform (441 amino acids), the predominant adult brain variant implicated in tauopathies, including Alzheimer's disease, was studied (3). The canonical tau structure was downloaded from the RCSB Protein Data Bank (PDB ID 6QJH), and all heteroatoms and water molecules were removed using UCSF ChimeraX (28). To model disease-relevant post-translational modifications (PTMs), phosphorylated, acetylated, and dual-modified tau variants were generated using Vienna-PTM (29). Phosphate groups were added to serine/threonine residues commonly hyperphosphorylated in tauopathies (S199, S202, T205, S214, S262, S396, S404). Acetyl groups were introduced at lysine residues located in microtubule-binding repeats and KXGS motifs that show pathological acetylation in tauopathies (K274, K280, K281, K290, K298). The dual-modified tau variant contained both sets of PTMs. All modified structures were energy-minimized before downstream analyses.

Aggregation and Flexibility Analysis

The aggregation propensity of native, phosphorylated, acetylated, and dual-modified tau was quantified using AGGRESCAN4D (30). This tool produces residue-level aggregation scores and 3D aggregation heatmaps. Each variant was analyzed in five independent runs, and mean aggregation values were used for comparison.

Protein flexibility was assessed using CABS-Flex 2.0 (14), which calculates per-residue root mean square fluctuation

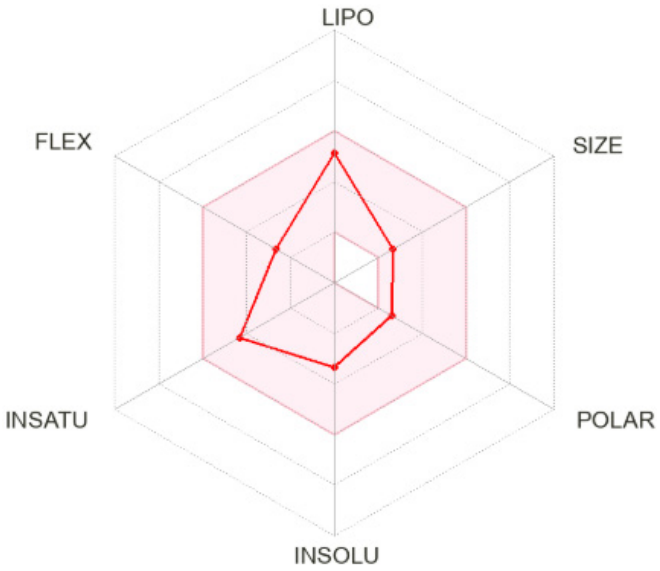

Figure 6: SwissADME radar plot of RI-GSK. Visualization of lipophilicity, polarity, molecular size, flexibility, saturation, and solubility parameters calculated for RI-GSK, all within optimal ranges (pink region) for CNS-active drugs. ADMET screening performed using SwissADME.

https://doi.org/10.59720/25-250

(RMSF) of a protein. RMSF profiles were generated for each tau variant to compare structural stability across PTM states, with a focus on the microtubule-binding repeats.

Retro-Inverso Peptide Design

RFdiffusion (15) was used to design a library of fifty retro-inverso peptides targeting two enzymatic pockets: the ATP-binding cleft of glycogen synthase kinase-3β (GSK3β; PDB: 1I09) and the acetyl-CoA/substrate-binding groove of the p300 histone acetyltransferase (HAT) domain (EP300; PDB: 3BIY).

All candidate peptides were energy-minimized prior to docking. Model confidence (pLDDT), sequence recoverability (MPNN), interface error scores, PTM interaction scores, and low RMSD were used to select the top ten candidates shown in **Table 1**.

Molecular Docking Simulations and Binding Energy Analysis

Docking simulations were performed using AutoDock Vina (16) within PyRx. Docking grids were centered on the GSK3β ATP-binding pocket and the catalytic site of p300. Each peptide-protein pair was docked in three replicates, and mean binding affinities (kcal/mol) were used for analysis.

To contextualize RI-GSK's performance against known modulators, five small-molecule compounds reported to influence GSK3β and/or p300 activity in tauopathies were docked: tideglusib, salsalate, EGCG, methylene blue, and curcumin. These molecules were selected because they have been tested in clinical trials for Alzheimer's disease and other tauopathies and have been documented to display inhibitory effects on GSK3β and/or p300 pathways (18).

Molecular Dynamics Simulations

The top ten peptide-protein complexes were evaluated using molecular dynamics (MD) simulations in OpenMM (19). Each complex was solvated in a cubic TIP3P water box with at least 10 Å of padding and neutralized with 0.15 M NaCl. The AMBER14SB force field was used. Particle Mesh Ewald (PME) was applied for long-range electrostatics with a 10 Å cutoff, and all hydrogen-containing bonds were constrained.

Five thousand steps of energy minimization were performed, followed by a two-stage equilibration starting with 200 ps NVT at 310 K with 10 $kcal \cdot mol^{-1} \cdot Å^{-2}$ restraints on backbone atoms and then 800 ps NPT at 310 K and 1 atm with gradually released restraints. Production simulations were run for 50 ns per replicate, with three replicates per complex. A 2 fs timestep and Langevin integrator (friction coefficient 1 ps^{-1}) were used. Trajectories were saved every 10 ps.

Trajectory analysis included backbone RMSD, per-residue RMSF, and hydrogen-bond and salt-bridge occupancy with key catalytic residues (GSK3β: Asp200, Cys199, Leu188; p300 HAT active-site residues). Binding free energy estimates were calculated using MM/GBSA from snapshots sampled every 100 ps.

Pharmacological Screening and Peptide Optimization

Pharmacological suitability of the top ten peptides was assessed using SwissADME (21) and ProTox-II (31). Predicted parameters included blood–brain barrier (BBB) permeability, lipophilicity, solubility, polarity, molecular weight, and toxicity class.

RI-GSK was optimized by introducing hydrophobic residues at solvent-exposed positions to improve BBB permeability and metabolic stability. Optimized variants were re-docked and re-evaluated to confirm maintained binding affinity to GSK3β and p300.

Statistical Analysis

All measurements are reported as mean ± standard deviation (SD). For comparisons between multiple groups, two-way analysis of variance (ANOVA) followed by Tukey's post-hoc multiple-comparisons test was performed to identify specific significant pairwise differences (adjusted $p < 0.01$).

Received: September 23, 2025
Accepted: December 22, 2025
Published: March 23, 2026

REFERENCES

1. Alzheimer's Association. "2024 Alzheimer's Disease Facts and Figures." *Alzheimer's & Dementia*, vol. 20, no. 4, 2024, pp. 700-789, https://doi.org/10.1002/alz.13935.
2. Wang, Y., and E. Mandelkow. "Tau in Physiology and Pathology." *Nature Reviews Neuroscience*, vol. 17, 2016, pp. 5-21, https://doi.org/10.1038/nrn.2015.1.
3. Avila, J., et al. "Role of Tau Protein in Both Physiological and Pathological Conditions." *Physiological Reviews*, vol. 84, no. 2, 2004, pp. 361-384, https://doi.org/10.1152/physrev.00024.2003.
4. Hernandez, F., J. J. Lucas, and J. Avila. "GSK3 and Tau: Two Convergence Points in Alzheimer's Disease." *Journal of Alzheimer's Disease*, vol. 33, 2013, pp. S141-S144, https://doi.org/10.3233/JAD-2012-129003.
5. Medina, M., and J. Avila. "New Perspectives on the Role of Glycogen Synthase Kinase-3 in Alzheimer's Disease." *International Journal of Alzheimer's Disease*, 2010, Article ID 279521, https://doi.org/10.4061/2010/279521.
6. Min, S.-W., et al. "Acetylation of Tau Inhibits Its Degradation and Contributes to Tauopathy." *Neuron*, vol. 67, no. 6, 2010, pp. 953-966, https://doi.org/10.1016/j.neuron.2010.08.044.
7. Cook, C., et al. "Acetylation of the KXGS Motifs in Tau Inhibits Microtubule Binding and Promotes Pathological Aggregation." *PLoS One*, vol. 9, no. 4, 2014, e95833, https://doi.org/10.1371/journal.pone.0095833.
8. Cohen, T. J., et al. "The Acetylation of Tau Inhibits Its Function and Promotes Pathological Tau Aggregation." *Nature Communications*, vol. 2, 2011, p. 252, https://doi.org/10.1038/ncomms1255.
9. Morris, M., et al. "Tau Post-Translational Modifications in Wild-Type and Human Amyloid Precursor Protein Transgenic Mice." *Nature Neuroscience*, vol. 18, no. 8, 2015, pp. 1183-1189, https://doi.org/10.1038/nn.4067.
10. Briggs, R., S. P. Kennelly, and D. O'Neill. "Drug Treatments in Alzheimer's Disease." *Clinical Medicine*, vol. 16, no. 3, 2016, pp. 247-253, https://doi.org/10.7861/clinmedicine.16-3-247.
11. Chorev, M., and M. Goodman. "A Dozen Years of Retro-Inverso Peptidomimetics." *Accounts of Chemical Research*, vol. 26, no. 5, 1993, pp. 266-273, https://doi.org/10.1021/ar00029a005.
12. Braak, H., and E. Braak. "Neuropathological Stageing of Alzheimer-Related Changes." *Acta Neuropathologica*,

vol. 82, no. 4, 1991, pp. 239-259, https://doi.org/10.1007/BF00308809.
13. von Bergen, M., et al. "Assembly of Tau Protein into Alzheimer Paired Helical Filaments Depends on a Local Sequence Motif ((306)VQIVYK(311)) Forming Beta Structure." *Proceedings of the National Academy of Sciences*, vol. 97, no. 10, 2000, pp. 5129-5134, https://doi.org/10.1073/pnas.97.10.5129.
14. Kuriata, A., et al. "CABS-flex 2.0: A Web Server for Fast Simulations of Flexibility of Protein Structures." *Nucleic Acids Research*, vol. 46, 2018, pp. W338-W343, https://doi.org/10.1093/nar/gky356.
15. Watson, J. L., et al. "De Novo Design of Protein Structure and Function with RFdiffusion." *Nature*, vol. 620, 2023, pp. 1089-1100, https://doi.org/10.1038/s41586-023-06415-8.
16. Trott, O., and A. J. Olson. "AutoDock Vina: Improving the Speed and Accuracy of Docking with a New Scoring Function, Efficient Optimization, and Multithreading." *Journal of Computational Chemistry*, vol. 31, no. 2, 2010, pp. 455-461, https://doi.org/10.1002/jcc.21334.
17. Panza, F., et al. "Tau-Centric Targets and Drugs in Clinical Development for the Treatment of Alzheimer's Disease." *BioMed Research International*, vol. 2016, 2016, Article ID 3245935, https://doi.org/10.1155/2016/3245935.
18. Ringman, J. M., et al. "A Potential Role of the Curry Spice Curcumin in Alzheimer's Disease." *Current Alzheimer Research*, vol. 2, no. 2, 2005, pp. 131-136, https://doi.org/10.2174/1567205053585882.
19. Eastman, P., et al. "OpenMM 8: Molecular Dynamics Simulation with Machine Learning Potentials." *Journal of Physical Chemistry B*, vol. 128, no. 1, 2024, pp. 109-116, https://doi.org/10.1021/acs.jpcb.3c06662.
20. Pajouhesh, H., and G. R. Lenz. "Medicinal Chemical Properties of Successful Central Nervous System Drugs." *NeuroRx*, vol. 2, no. 4, 2005, pp. 541-553, https://doi.org/10.1602/neurorx.2.4.541.
21. Daina, A., O. Michielin, and V. Zoete. "SwissADME: A Free Web Tool to Evaluate Pharmacokinetics, Drug-Likeness and Medicinal Chemistry Friendliness of Small Molecules." *Scientific Reports*, vol. 7, 2017, Article 42717, https://doi.org/10.1038/srep42717.
22. Guo, T., et al. "Roles of Tau Protein in Health and Disease." *Acta Neuropathologica*, vol. 133, no. 5, 2017, pp. 665-704, https://doi.org/10.1007/s00401-017-1707-9.
23. Johnson, G. V., and W. H. Stoothoff. "Tau Phosphorylation in Neuronal Cell Function and Dysfunction." *Journal of Cell Science*, vol. 117, 2004, pp. 5721-5729, https://doi.org/10.1242/jcs.01558.
24. Tracy, T. E., et al. "Acetylated Tau Obstructs KIBRA-Mediated Signaling in Synaptic Plasticity and Promotes Tauopathy-Related Memory Loss." *Neuron*, vol. 90, no. 2, 2016, pp. 245-260, https://doi.org/10.1016/j.neuron.2016.03.005.
25. Alquezar, C., et al. "Targeting Tau Phosphorylation by Imidazole-Based Compounds: A Drug Repurposing Strategy for Alzheimer's Disease and Related Tauopathies." *Scientific Reports*, vol. 6, 2016, Article 33336, https://doi.org/10.1038/srep33336.
26. Li, L., et al. "Tau Ubiquitination in Alzheimer's Disease." *Frontiers in Neurology*, vol. 12, 2022, Article 786353, https://doi.org/10.3389/fneur.2021.786353.
27. Chinnathambi, S., and N. Rangappa. "SUMO Inhibits Tau Aggregation in Alzheimer's Disease." *Advances in Protein Chemistry and Structural Biology*, vol. 147, 2025, pp. 355-374, https://doi.org/10.1016/bs.apcsb.2025.02.001.
28. Pettersen, E. F., et al. "UCSF Chimera—A Visualization System for Exploratory Research and Analysis." *Journal of Computational Chemistry*, vol. 25, no. 13, 2004, pp. 1605-1612, https://doi.org/10.1002/jcc.20084.
29. Margreitter, C., D. Petrov, and B. Zagrovic. "Vienna-PTM Web Server: A Toolkit for MD Simulations of Protein Post-Translational Modifications." *Nucleic Acids Research*, vol. 41, 2013, pp. W422-W426, https://doi.org/10.1093/nar/gkt364.
30. Zalewski, M., et al. "Aggrescan4D: A Comprehensive Tool for pH-Dependent Analysis and Engineering of Protein Aggregation Propensity." *Protein Science*, vol. 33, no. 10, 2024, e5180, https://doi.org/10.1002/pro.5180.
31. Banerjee, P., et al. "ProTox 3.0: A Webserver for the Prediction of Toxicity of Chemicals." *Nucleic Acids Research*, vol. 52, no. W1, 2024, pp. W513-W520, https://doi.org/10.1093/nar/gkae303.